Cardiovascular Drugs and Therapy (2019) 33:25–33
https://doi.org/10.1007/s10557-018-6844-4

ORIGINAL ARTICLE

The Role of Tauroursodeoxycholic Acid on Dedifferentiation of Vascular Smooth Muscle Cells by Modulation of Endoplasmic Reticulum Stress and as an Oral Drug Inhibiting In-Stent Restenosis

Hangqi Luo[1,2] · Changzuan Zhou[3] · Jufang Chi[1] · Sunlei Pan[4] · Hui Lin[1] · Feidan Gao[1] · Tingjuan Ni[1] · Liping Meng[1] · Jie Zhang[1] · Chengjian Jiang[1] · Zheng Ji[1] · Haitao Lv[1] · Hangyuan Guo[1]

Published online: 21 January 2019

Abstract

Purpose The role of endoplasmic reticulum (ER) stress in cardiovascular disease is now recognized. Tauroursodeoxycholic acid (TUDCA) is known to have cardiovascular protective effects by decreasing ER stress. This study aimed to assess the ability of TUDCA to decrease ER stress, inhibit dedifferentiation of vascular smooth muscle cells (VSMCs), and reduce in-stent restenosis.

Methods The effect of TUDCA on dedifferentiation of VSMCs and ER stress was investigated in vitro using wound-healing assays, MTT assays, and western blotting. For in vivo studies, 18 rabbits were fed an atherogenic diet to induce atheroma formation. Bare metal stents (BMS), BMS+TUDCA or Firebird stents were implanted in the left common carotid artery. Rabbits were euthanized after 28 days and processed for scanning electron microscope (SEM), histological examination (HE), and immunohistochemistry.

Results In vitro TUDCA (10–1000 μmol/L) treatment significantly inhibited platelet-derived growth factor (PDGF)-BB-induced proliferation and migration in VSMCs in a concentration-dependent manner and decreased ER stress markers (IRE1, XBP1, KLF4, and GRP78). In vivo, we confirmed no significant difference in neointimal coverage on three stents surfaces; neointimal was significantly lower with BMS+TUDCA (1.6 ± 0.2 mm^2) compared with Firebird (1.90 ± 0.1 mm^2) and BMS (2.3 ± 0.1 mm^2). Percent stenosis was lowest for BMS+TUDCA, then Firebird, and was significantly higher with BMS ($28 \pm 4\%$, $35 \pm 7\%$, $40 \pm 1\%$; respectively; $P < 0.001$). TUDCA treatment decreased ER stress in the BMS+TUDCA group compared with BMS.

Conclusions TUDCA inhibited dedifferentiation of VSMCs by decreasing ER stress and reduced in-stent restenosis, possibly through downregulation of the IRE1/XBP1 signaling pathway.

Keywords Vascular smooth muscle cells · Tauroursodeoxycholic acid · Dedifferentiation · In-stent restenosis · Endoplasmic reticulum stress · IRE1/XBP1 signaling pathway

Introduction

Drug-eluting stents (DES) have replaced bare metal stents (BMS) in percutaneous coronary intervention (PCI) because DES have lower in-stent restenosis rates [1–3] Compared with BMS, optimizations such as the use of polymers and determination of both optimal drug dosing and release kinetics have led to better clinical outcomes for DES. At present, there are many types of DES in clinical use, such as everolimus-eluting stents, paclitaxel-eluting stents, and sirolimus-eluting stents among others [4–7]. However, there are still signs of late stent failure, such as late stent thrombosis and restenosis with the use of these improved stents [8–11]. Published clinical

✉ Hangyuan Guo
guohangyuan@yeah.net

[1] Department of Cardiology, Shaoxing People's Hospital (Shaoxing Hospital, Zhejiang University School of Medicine), No. 568 Zhongxing North Road, Shaoxing, Zhejiang, China

[2] Zhejiang University School of Medicine, Zhejiang, Hangzhou, China

[3] Department of Cardiology, Wenzhou City Hospital of Traditional Chinese Medicine and Western Medicine Combined, Wenzhou, Zhejiang, China

[4] Department of Cardiology, The First Affiliated Hospital, Wenzhou Medical University, Wenzhou, Zhejiang, China

statistics indicate that the probability of stent restenosis increases significantly in patients with a DES after 24 months [12]. Although biodegradable stents have recently been developed and marketed for stent restenosis, it takes a long time for these scaffold materials to be completely absorbed. Compared with previous stents, biodegradable stents are thicker, which can easily cause local blood flow disorders and thrombus formation [13]. Existing methods to prevent the occurrence of stent restenosis are unsatisfactory. Strategies to further inhibit stent restenosis are needed. Unraveling the mechanisms involved in vascular smooth muscle cell (VSMC) phenotypic switch is an important step towards gaining a better understanding of the pathophysiology of these disorders and ultimately determining effective strategies for their treatment and prevention.

Mature, normal VSMCs are highly specialized cells with differentiated, resting, and contracted phenotypes; they exhibit elevated levels of contractile proteins, such as α-smooth muscle actin (α-SMA) and calmodulin (Cal). The destruction of local intimal integrity and the exposure of the muscular layer after interventional treatment cause local platelet aggregation and the release of platelet-derived growth factor (PDGF) and inflammatory factors, which strongly induce dedifferentiation of VSMCs and their migration to the lumen. In the present study, PDGF-BB was selected to induce VSMC dedifferentiation in vitro.

Tauroursodeoxycholic acid (TUDCA), a conjugated bile acid, has been used effectively for the treatment of primary sclerosing cholangitis and primary biliary cirrhosis [14–17]; the mechanism of action of TUDCA is attenuation of endoplasmic reticulum (ER) stress. Because TUDCA has various regulatory cell functions, namely, anti-inflammatory and immunomodulatory effects [18], many studies have investigated the potential of TUDCA in the treatment of extrahepatic diseases [19]. Cho JG et al. reported that TUDCA promoted blood vessel repair by recruiting vasculogenic progenitor cells [20]. Ma J et al. reported that TUDCA inhibited iNOS expression to protect cardiovascular cells [21]. It also has been reported that TUDCA could be used to prevent isolated cardiac ischemia and reperfusion injury [22]. Adjuvant treatment of TUDCA has been shown to reduce the incidence of acute cardiac allograft rejection. Kim SY et al. indicated that TUDCA suppressed neointimal hyperplasia after vascular injury [23].

The effect of TUDCA on modulation of VSMC dedifferentiation and ER stress remains unknown and the role of TUDCA in inhibiting in-stent restenosis has not been confirmed. In this study, we tested whether TUDCA treatment could interfere with PDGF-BB-induced proliferation and migration of VSMCs. We also investigated the effect of TUDCA on ER stress markers, IRE1, XBP1, KLF4, and GRP78 in vitro. TUDCA was tested in vivo to determine a potential role in inhibiting in-stent restenosis. Our study will help to evaluate the potential use of TUDCA as a new DES.

Methods

Cell Culture and Identification Rat VSMCs were isolated from thoracic aortas of male SD rats using an improved tissue-sticking method developed in our previous studies, then cultured in Dulbecco's modified Eagle's medium (DMEM) containing 10% fetal bovine serum (FBS) at 37 °C in a humid atmosphere with 5% CO_2. Immunocytochemical detection of the contractile marker protein α-SMA was used to identify primary VSMCs. VSMCs were cultured to 70–80% confluency (passage numbers 4–7) and serum-starved overnight before use in experiments. Cells were then pretreated with different concentrations of TUDCA (1 μmol/L, 10 μmol/L, and 100 μmol/L, respectively) for 24 h before 24 h incubation with PDGF-BB (20 ng/mL).

Atherosclerotic Rabbit Model Stent Implantation Protocols used for all animal studies were approved by the Zhejiang University Animal Policy and Welfare Committee and complied with the NIH guidelines (Guide for the Care and Use of Laboratory Animals).

New Zealand White Rabbits (2.0–3.0 kg, Dashi Juxin Rabbit Farms, Xinchang Country, Zhejiang Province, China) were randomly divided into three groups: BMS ($n = 6$; BMS, Mluti-Link Vision, Abbott Vascular, USA), BMS+TUDCA ($n = 6$; BMS, Mluti-Link Vision, Abbott Vascular, USA; TUDCA, Taurolite, Bruschettini S.R.L, Genova, Italy), Firebird ($n = 6$; Firebird, MicroPort, China). All rabbits were fed a high fat and cholesterol diet (1% cholesterol, 5% peanut oil, and 10% egg yolk powder) to induce atheroma formation (atherogenic diet). After 1 week of feeding the atherogenic diet, the rabbits were anesthetized with 4 mg/kg of 4% chloral hydrate solution injected into their ear veins. After the left external carotid artery was exposed, a 5F Fogarty embolectomy catheter was introduced through an external carotid arteriotomy incision, advanced to the common carotid artery, and BMS or Firebird stents were implanted. The BMS+TUDCA group was given 100 mg/kg oral TUDCA for 28 days [23]. All animals received postoperative 40 mg aspirin and 70 mg Ticagrelor daily. Firebird is the first generation of domestic DES produced by MicroPort and approved by State Food and Drug Administration (SFDA). The surface of Firebird is evenly coated with rapamycin and the polymer that controls rapamycin release. It has been used extensively in China and many studies have shown that Firebird can reduce the incidence of in-stent restenosis [24–26]; Firebird was used as a positive control in our experiments.

Euthanasia and Fixation After stent implantation, animals were maintained on an atherogenic diet for an additional 28 days (total of 5 weeks). At the end of the 5 weeks, the rabbits underwent overnight fasting, then were anesthetized with 4 mg/kg of 4% chloral hydrate solution in their ear veins.

The rabbit's neck skin was incised, and the left common carotid artery was obtained and perfused at 80 mmHg (dripping from a height of %2 m) with Ringer's lactate until the perfusate from the jugular vein was clear of blood.

Scanning Electron Microscopy The stented arterial segments were fixed in glutaraldehyde solution and longitudinally bisected to expose the luminal surface and then photographed. A scanning electron microscope (SEM) was used to observe the cell coverage on the surface of the stents at incremental magnifications of × 30, × 1000, and × 3000.

Immunohistochemistry Tissue samples of stented arterial segments preserved in 10% formalin solution were dehydrated and embedded in paraffin using standard methods. The paraffin sections were deparaffinized using standard methods then immersed in distilled water. Paraffin sections were then rinsed in phosphate buffered solution with Tween (PBS-T, 3 × 5 min) and blocked with 3% peroxide-methanol at room temperature for endogenous peroxidase ablation. All of the following steps were carried out in a moist chamber. Tissues were first incubated with blocking buffer (normal goat serum) at room temperature for 20 min, goat serum was then discarded and primary antibody diluted in PBS (0.01 M PBS, pH 7.4) was added, the tissues were incubated overnight at 4 °C. Next, tissues were rinsed in PBS-T (3 × 5 min) and incubated with horse radish peroxidase (HRP)-conjugated secondary antibody at 37 °C for 30 min. Tissues were next rinsed in PBS-T (3 × 5 min) and the color was developed using 3,3-diaminobenzidine (DAB) for 10 min at room temperature in the dark. After coloration, tissues were rinsed with the distilled water and processed for hematoxylin staining, dehydration, clearing and mounting with neutral gums. Finally, the tissue samples were evaluated using a microscope (Leica DM3000 Germany). The specific antibodies used in this study were: anti-α-SMA (Abcam, ab21027), anti-IRE1 (Abcam, ab48187), anti-XBP1 (Abcam, ab37152), anti-KLF4 (Abcam, ab215036), anti-GAPDH (Abcam, ab8245), HRP-conjugated goat anti-rabbit (Gene Tech, GK500710), and HRP-conjugated goat anti-mouse (Gene Tech, GK500710).

Histological Evaluation Stented sections were stained with hematoxylin and eosin. Cross-sectional areas (stent area and lumen) of each section were measured using digital morphometry. Percentages of stenosis were calculated using the following formulas: (neointimal volume) = (stent area) − (lumen) and (percentage stenosis) = (neointimal volume) / (stent area) × 100(%). Inflammation and foamy macrophage infiltration within the neointimal (representing neoatherosclerosis) were examined on hematoxylin and eosin stained sections of each stent part (proximal, middle, distal).

MTT Assay VSMCs that were between passages 3 and 7 were serum-starved overnight followed by 0.25% trypsin digestion of the cell monolayer. DMEM (high-glucose) containing 10% FBS was added to the cell suspension then the cells were counted. Each well was seeded with 5×10^4 cells (in 200 μL) in a 96-well culture plate. In the experimental group, cells were pretreated with different TUDCA concentrations (1 μmol/L, 10 μmol/L or 100 μmol/L) for 24 h then PDGF-BB (20 ng/mL) was added for 12, 24, or 48 h. In the control group, cells were cultured without any treatment. In the PDGF-BB group, cells were treated only with PDGF-BB (20 ng/mL, 12, 24, or 48 h). Both experimental and control groups were cultured at 37 °C with 5% CO_2. After treatment, MTT solution (20 μL) was added and the cells were incubated for 4 h. Next, the medium was carefully removed and 150 μL DMSO was added to each well followed by gentle rotation on an orbital shaker for 10 min at room temperature. A microplate reader (Bio-Rad, Hercules, CA, USA) was used to determine absorbance at 490 nm.

Wound-Healing Assay VSMCs were cultured to 90% confluence, serum-starved, then treated with hydroxyurea overnight for synchronization and growth inhibition. A wound was created in the VSMC monolayer using a sterile 100-μL pipette tip. PBS was used to flush the 6-well plate and wash away cell debris. After addition of various test articles, cells were analyzed at 0 and 24 h post-wounding using a Nikon microscope (Nikon Corporation, Tokyo, Japan) equipped with Image-pro plus 6.0 software (Media Cybernetics Inc., Bethesda, MD, USA). The ratio of cell recovery area to whole wound area was used to evaluate cell migration.

Western Blot VSMCs were grown in DMEM with 10% FBS. Before processing the cells for Western blot, the culture medium was removed and cells were washed three times with PBS. VSMCs were then lysed with lysis buffer (Beyotime, Haimen, China) on ice for 30 min followed by ultrasonication. Cell lysates were centrifuged at 12,000×*g* for 15 min at 4 °C. Equal amounts of soluble protein were separated by 12% SDS-PAGE and protein bands were electro-transferred onto polyvinylidene fluoride membranes. The membranes were blocked with 5% skim milk, followed by primary antibody incubation overnight. Secondary antibodies conjugated with HRP were used in these experiments. An ECL chemiluminescence detection kit was used to visualize the target proteins as well as the internal control. Protein bands were obtained by autoradiography and analyzed by Quantity One 4.4 (Bio-Rad, Hercules, CA, USA). The specific antibodies used in this study were: anti-α-SMA (Abcam, ab21027), anti-Cal (Abcam, ab45689), anti-osteopontin (OPN) (Abcam, ab8448), anti-IRE1 (Abcam, ab48187), anti-XBP1 (Abcam, ab37152), anti-KLF4 (Abcam, ab215036), anti-GAPDH (Abcam, ab8245), HRP-conjugated goat anti-rabbit

(Beoyotime, A0208) and HRP-conjugated goat anti-mouse (Beoyotime, A0216).

Statistical Analysis Each in vitro experiment was repeated at least three times using a fresh batch of cells for each experiment. SPSS 19.0 statistical software (SPSS Inc., Chicago, IL, USA) was used to perform statistical analyses. Data are expressed as means ± standard deviation (SD). Multiple group comparisons were achieved using a one-way analysis of variance (ANOVA), followed by Bonferroni post-hoc tests. Unpaired Student's *t* test was used for two-group comparisons. The BMS group was used as a control and compared with various DES groups. $P < 0.05$ was considered statistically significant.

Results

VSMC Identification Most VSMCs in primary cell culture show a contractile phenotype with a long spindle or spindle appearance. The contractile phenotype of VSMCs mainly expresses α-SMA, calponin1, and smooth muscle myosin heavy chain. Logarithmic phase VSMCs showed "peak" and "valley" growth, were positive for α-SMA immunocytochemical staining and had abundant filamentous parallel staining in the cytoplasm which was distributed along the longitudinal axis of the cells. Nuclear counterstaining was performed using DAPI.

TUDCA Inhibited PDGF-BB-Induced VSMC Dedifferentiation VSMCs were pretreated with 1, 10, or 100 mmol/L TUDCA then stimulated with PDGF-BB (20 ng/mL) for 24 h. PDGF-BB-induced VSMC proliferation and migration was inhibited in cells pretreated with TUDCA compared with those that were not in wound-healing and MTT assays. This inhibition was concentration-dependent (Fig. 1a, b; $P < 0.05$).

TUDCA May Inhibit PDGF-BB-Induced VSMC Dedifferentiation via IRE1/XBP1 Signaling VSMCs pretreated with 0, 1, 10, or 100 mmol/L of TUDCA followed by stimulation with PDGF-BB (20 ng/mL) for 48 h were processed for western blotting. Western blot results showed that VSMCs reduced α-SMA and Cal protein expression levels but increased OPN protein expression in the PDGF-BB group compared with the control group, which indicates that PDGF-BB induced dedifferentiation of VSMCs. The expression levels of α-SMA and Cal protein were increased and OPN was reduced in cells that received PDGF-BB and were pretreated with TUDCA. These results indicate that TUDCA inhibited PDGF-BB-induced VSMC dedifferentiation in a concentration-dependent manner (Fig. 2, $P < 0.05$).

To further explore the cellular mechanisms by which TUDCA inhibits PDGF-BB-induced VSMC dedifferentiation, we measured the ER stress markers IRE1, XBP1, KLF4, and GRP78. As shown in Fig. 3, IRE1, XBP1, KLF4, and GRP78 proteins levels in TUDCA group VSMCs were significantly lower than those in the PDGF-BB-induced group; this effect was concentration-dependent (Fig. 3, $P < 0.05$). These results indicate that TUDCA inhibited PDGF-BB-induced VSMC dedifferentiation by decreasing ER stress and that the mechanism may involve down-regulation of the IRE1/XBP1 signaling pathway.

Scanning Electron Microscopy, Histological Evaluation, and Immunohistochemistry New Zealand rabbits fed an atherogenic diet were implanted with BMS, BMS+TUDCA or

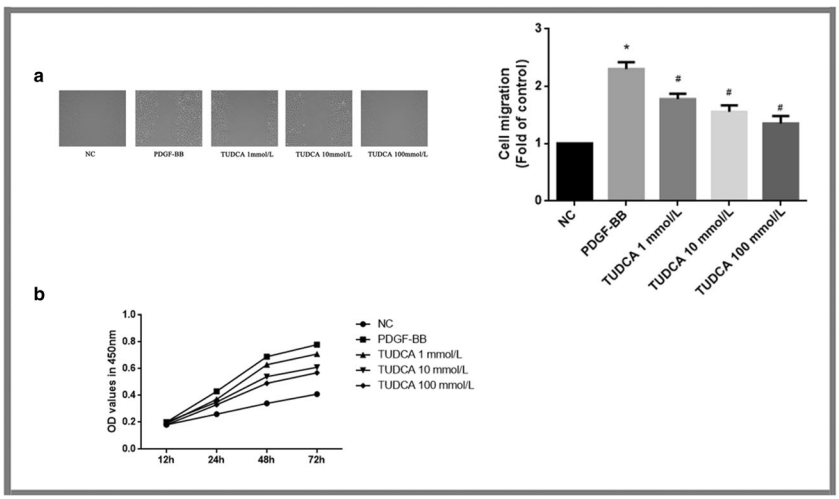

Fig. 1 Taurousodeoxycholic acid inhibits PDGF-BB-induced VSMC dedifferentiation. Control, VSMCs were cultured without any treatment; PDGF-BB, VSMCs were treated only with PDGF-BB (20 ng/mL); Tauroursodeoxycholic acid, VSMCs were pretreated with variousconcentrations (1, 10, and 100 μmol/L) of tauroursodeoxycholic acid followed by stimulation with PDGF-BB (20 ng/mL) for 24 h. **a** Wound-healing assay was employed to evaluate migrationin VSMCs (*$P < 0.05$ vs control group; $^{\#}P < 0.05$ vs treatment with PDGF-BB alone; $n = 3$). **b** MTT assay was used to assess the proliferation of VSMCs

Firebird stents in the left common carotid arteries. Vessels with stents were removed 4 weeks later for SEM, histological evaluation (HE), and immunohistochemistry.

SEM showed that all stent struts had been completely covered by endothelial cells and the stent struts could be seen from the cross section of the blood vessel (Fig. 4a). The panel insets are representative images from proximal and distal regions showing endothelial cells, smooth muscle cells, surface thrombi and inflammatory cells with an increased SEM magnification (Fig. 4b).

Representative HE images for four BMS, five BMS+TUDCA and five Firebird stents harvested from rabbits euthanized at 28 days are shown in Fig. 5. Two rabbits died of infection and one rabbit died from an unknown cause (possibly an embolism). All stent types showed various extents of inflammation and neoatherosclerosis. Morphometric analysis revealed that the stent area was bigger in the Firebird group compared with both BMS and BMS+TUDCA (stent area: Firebird 6.1 ± 0.3 mm^2, BMS 5.7 ± 0.2 mm^2, BMS+TUDCA 5.8 ± 0.2 mm^2; $P < 0.001$) (Table 1). In contrast, the neointimal area was the largest in animals with a BMS, followed by Firebird and BMS+TUDCA; the difference in the neointimal area of the three groups were statistically significant (stent area: Firebird 1.9 ± 0.1 mm^2, BMS 2.3 ± 0.1 mm^2, BMS+TUDCA 1.6 ± 0.2 mm^2; $P < 0.001$) (Table 1). The percentage of restenosis was highest in the BMS group and lowest in the BMS+TUDCA group (stent area: Firebird $35 \pm 7\%$, BMS $40 \pm 1\%$ BMS+TUDCA $28 \pm 4\%$; $P < 0.001$).

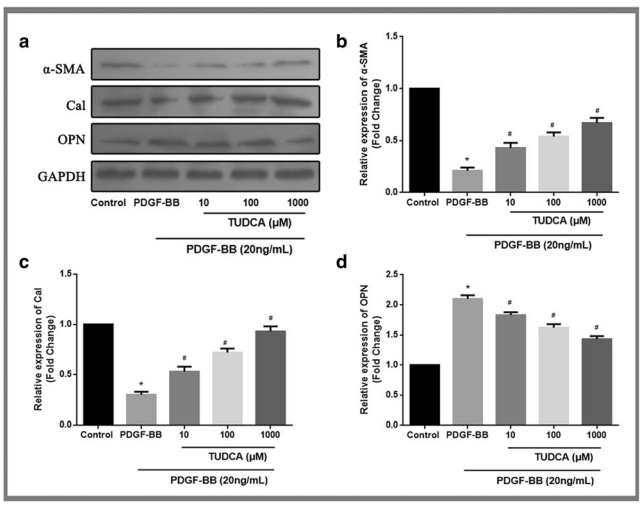

Fig. 2 Taurousodeoxycholic acid inhibits PDGF-BB-induced VSMC dedifferentiation. Control, VSMCs were cultured without any treatment; PDGF-BB, VSMCs were treated only with PDGF-BB (20 ng/mL); Tauroursodeoxycholic acid, VSMCs were pretreated with various concentrations (1, 10, and 100 μmol/L) of tauroursodeoxycholic acid followed by stimulation with PDGF-BB (20 ng/mL) for 24 h. **a**, **b**, **c**, **d** Western blot was employed to quantitate the expression levels of contractile proteins (*$P < 0.05$ vs control group; $^{\#}P < 0.05$ vs treatment with PDGF-BB alone; $n = 3$)

We also showed that in the atherosclerotic rabbit model, VSMCs dedifferentiate. Immunohistochemistry showed that the BMS group had a reduced expression level of α-SMA and an increased expression level of IRE1, XBP1, KLF4, and GRP78 proteins compared with the other two groups. In the BMS+TUDCA and Firebird groups, the expression level of IRE1, XBP1, and KLF4 were decreased, while the expression level of α-SMA was increased. TUDCA and rapamycin could inhibit the dedifferentiation of VSMCs (Fig. 6).

Discussion

PCI reduces the mortality rate of myocardial infarction. The purpose of stent implantation is to resolve stenosis and save patients with acute myocardial infarction. However, over time, in-stent restenosis has become a common problem. Studies have shown that in patients with DES, the 10-year stent restenosis is approximately 22%. Repeated stent implantation not only increases the financial burden for the patient but also threatens the patient's life. Therefore, it is necessary to fully understand the mechanism of in-stent restenosis so new drugs that can inhibit in-stent restenosis can be identified or more effective DESs can be designed.

Owen et al. used cell lineage tracing technology to show that VSMCs formed more than 80% of the intimal hyperplasia; this finding improved our understanding of the importance of VSMCs in vascular diseases [27]. Dedifferentiation of VSMCs is a key event in the development of atherosclerosis as it inhibits VSMC phenotype switching, reduces the proliferation and migration of the VSMCs and is an effective way to reduce neointimal hyperplasia and inhibit in-stent restenosis. It is well known that shear stress regulates the proliferation and migration of VSMCs through mechanisms that involve PDGF and matrix metalloproteinase-2 (MMP-2) through the nitric oxide signaling pathway [28–31]. PDGF-BB can transition VSMCs from a differentiated to a dedifferentiated phenotype [32]. In vitro, we found that PDGF-BB induced proliferation and migration in smooth muscle cells and reduced the levels of differentiation-specific contractile proteins α-SMA and Cal. In vivo, an atherosclerotic rabbit model showed that the level of the differentiation-specific contractile protein α-SMA was lowest in the BMS group; conversely, the expression of α-SMA in BMS+TUDCA and Firebird stents was increased.

TUDCA is a hydrophilic bile acid and has been used in the clinic for many years to treat a variety of liver diseases including the dissolution of gallstones and hepatitis C viral infection [14, 33, 34] and has been shown to be quite safe. Kim et al. reported that TUDCA can reduce neointimal hyperplasia by decreasing ER stress [23]. ER stress occurs in cells that are affected by abnormal environmental stimuli which results in instability of the intracellular environment, increased

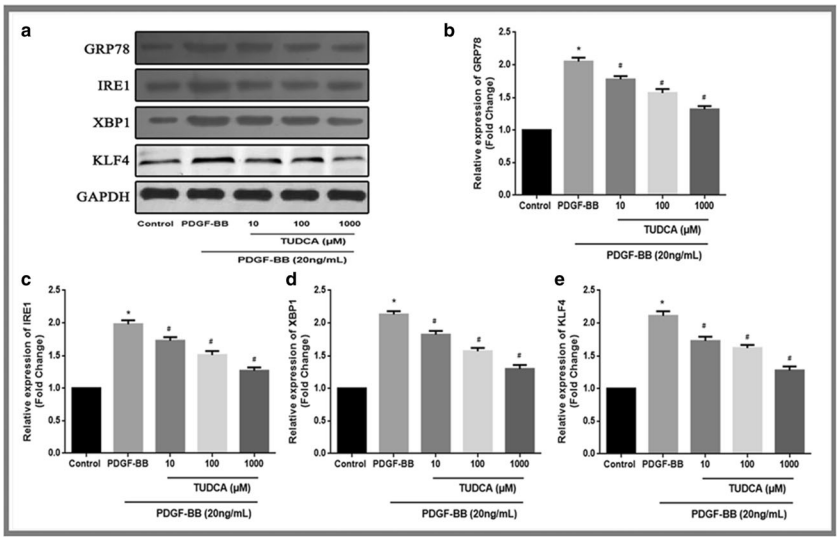

Fig. 3 Taurousodeoxycholic acid inhibits PDGF-BB-induced VSMC dedifferentiation via IRE1/XBP1 signaling. Control, VSMCs were cultured without any treatment; PDGF-BB, VSMCs were treated only with PDGF-BB (20 ng/mL); Tauroursodeoxycholic acid, VSMCs were pretreated with various concentrations (1, 10 and 100 μmol/L) of tauroursodeoxycholic acid followed by stimulation with PDGF-BB (20 ng/mL) for 24 h. **a**, **b**, **c**, **d**, **e** Western blotting was applied to assess IRE1, XBP1, KLF4, GRP78 protein levels in VSMCs treated with various concentrations of tauroursodeoxycholic acid followed by stimulation with PDGF-BB. Tauroursodeoxycholic acid treatment resulted in IRE1, XBP1, KLF4, and GRP78 protein levels significantly lower compared with PDGF-BB group values, in a concentration-dependent manner. ($^{*}P < 0.05$ vs control group; $^{\#}P < 0.05$ vs treatment with PDGF-BB alone; $n = 3$)

misfolded or unfolded polypeptide chains and a decline in the ER folding function, ultimately causing an abnormal accumulation of non-functional proteins in the lumen of the ER. ER stress can induce a self-protection reaction in the cell, unfolded protein response (UPR) activation, which can activate three distinct ER membrane-spanning signal molecules, namely, IRE1, PKR-like ER kinase (PERK), and activating transcription factor 6 (ATF6) [35]. Some studies indicate that TUDCA is a potent reducer of ER stress [35–37], Hua Y et al. reported that TUDCA activated all three UPR pathways (PERK, IRE1, and ATF6) [35]. Consistent with previous reports, our study showed that TUDCA activated one of the URP pathways, IRE1, resulting in reduced expression of IRE1 in both in vitro and in vivo experiments, while the levels of anti-tubulin, α-SMA, and Cal were increased.

As an important transcription factor in ER stress, XBP1 plays a key role in disease. XBP1 mRNA is full-length in the absence of ER stress and is generally considered not to have a translation function. However, ER stress activates IRE1 cleavage enzyme activity which induces a 26-base deletion of XBP1 mRNA. This smaller mRNA is transcribed and translated into a functional XBP1 protein [38]. Zeng

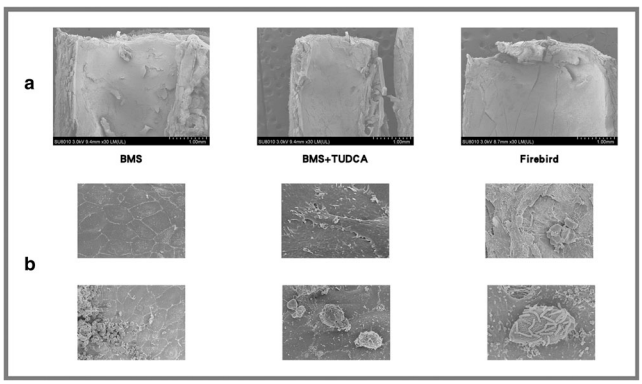

Fig. 4 The upper panels show corresponding radiographic images of each stent. **a** The surfaces of the three stents (BMS, BMS+TUDCA, Firebird) are covered by endothelial cells. **b** The panel insets are representative images at higher magnification (× 3500) from proximal and distal regions showing thrombi, inflammatory cells, and endothelial cells. The pictures of endothelial cells, smooth muscle cells, surface thrombi, and inflammatory cells after magnified the shooting multiple of SEM

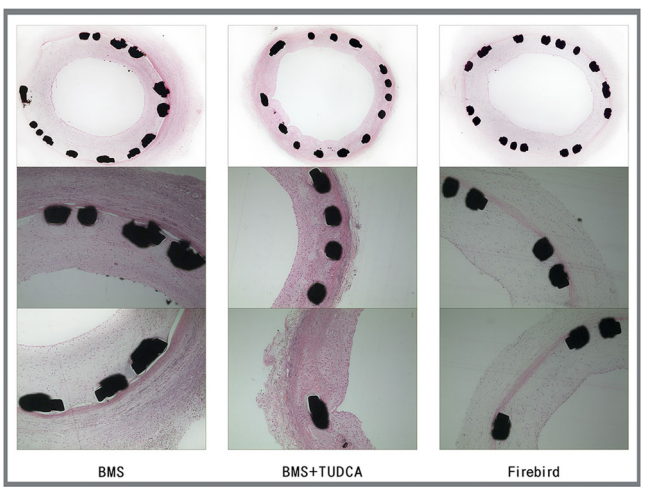

Fig. 5 Representative histological images of 4 BMS, 5 BMS+ TUDCA, and 5 Firebird stents harvested from animals euthanized at 28 days. All stent types showed various extents of inflammation and neoatherosclerosis

Table 1 Characteristics of tested stents

Variable	BMS ($n = 4$)	BMS+TUDCA ($n = 5$)	Firebird ($n = 5$)
Stent area (mm^2)	5.7 ± 0.2	5.8 ± 0.2	6.1 ± 0.3
Neointima (mm^2)	2.3 ± 0.1	1.6 ± 0.2	1.9 ± 0.1
Stenosis (%)	40 ± 1	28 ± 4	35 ± 7

et al. observed that XBP1 was particularly highly expressed in plaque-prone areas such as bifurcation or flexion, and overexpression of XBP1 aggravated aortic plaque progression in Apoe−/− mice and promoted intimal hyperplasia [39]. Xv Q et al. found that XBP1 in the damaged arterial region was significantly higher in mice subjected the arterial injury mouse model and that inhibiting the expression of XBP1 in the injured area could significantly reduce intimal hyperplasia [39]. Consistent with these reports, the present study indicated that in vivo XBP1 was significantly elevated in the atherosclerotic plaque area, and that expression of XBP1 in the BMS group was higher than that in the BMS+TUDCA and Firebird groups. In the in vitro study, TUDCA inhibited the expression of XBP1.

Mosbah et al. reported that TUDCA could activate all three branches of UPR and their downstream targets, as well as inducing ER stress, evidenced by CHOP and GRP78 upregulation. Consistent with this report, this study demonstrated that TUDCA reduced the proliferation and migration of VSMCs induced by PDGF-BB and that TUDCA inhibited dedifferentiation of VSMCs [40]. In addition, TUDCA reduced expression of GRP78 in both in vitro and in vivo studies. Interestingly, we found that KLF4 had the same expression pattern as IRE1 and XBP1. KLF4, IRE1, and XBP1 are likely to interact in VSMCs and affect the phenotype of these cells in in-stent restenosis.

With DES reducing the rates of in-stent restenosis, there is a concern about the increased risks of late stent thrombosis related to delayed endothelialization [9, 41, 42]. Causes of late stent thrombosis include strut malapposition [43], longer stent, and longer lesion length [11] and drug inhibition. In the present study, the stent surfaces in the BMS+TUDCA and Firebird groups were covered by endothelial cells, and there was no significant difference compared with the BMS group. To our surprise, in the BMS+TUDCA group, the neointimal area was smaller than that in the BMS and Firebird groups; the percentage of stenosis was also significantly lower in the BMS+TUDCA group than in the BMS and Firebird groups. Sufficient neointimal hyperplasia can easily lead to in-stent restenosis while deficient neointimal hyperplasia can easily lead to late thrombosis. Our study showed that TUDCA could achieve a good balance between in-stent restenosis and late thrombosis.

As with all preclinical studies using animals, rabbit common carotid artery models may not adequately represent the biological response of atherosclerotic arteries in humans. In our study, there was no significant difference in the coverage of endothelium among three groups, so the ability of TUDCA to inhibit early intimal hyperplasia could not be compared. Because of limited technology and funding, we could not produce a TUDCA-DES, which limits the interpretation of

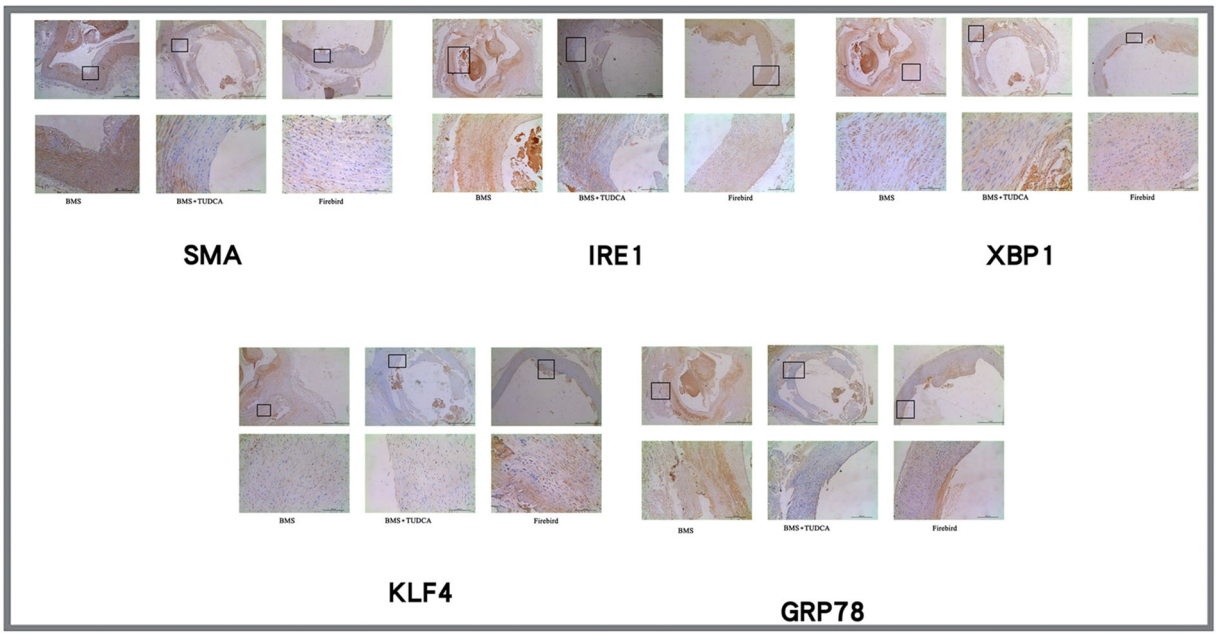

Fig. 6 Tauroursodeoxycholic acid has the same inhibitory effect on PDGF-BB-induces VSMC dedifferentiation as rapamycin. **a**, **b**, **c**, **d**, and **e** In BMS, the expression of SMA in blood vessels decreased, and the expression of IRE1, XBP1, KLF4, and GRP78 increased. In contrast, in BMS+TUDCA and Firebird, the expression of SMA increased in blood vessels, IRE1, XBP1, KLF4, and GRP78 expression decreased

our study. In this study, we used two different DESs, applying different stent platforms that may also have an impact on the final experimental results. Finally, the role of TUDCA in reducing ER stress through the IRE1/XBP1 pathway needs further confirmation.

Conclusion

Treatment with TUDCA in vitro significantly inhibited the proliferation and migration of VSMCs and decreased multiple ER stress markers (IRE1, XBP1, KLF4, and GRP78), which may indicate the involvement of the IRE1/XBP1 signaling pathway. Furthermore, in vivo, the BMS+TUDCA group showed the lowest percentage of stenosis compared with the Firebird and BMS groups.

Acknowledgments The authors thank the Faculty of Agriculture, Life and Environment Science at Zhejiang University for their valuable technical assistance. We thank Sarah Bubeck, Ph.D., from Liwen Bianji, Edanz Editing China (www.liwenbianji.cn/ac), for editing the English text of a draft of this manuscript.

Funding This study was supported by Co construction of Provincial Department key project (Grant No. WKJ-ZJ-1729) and Zhejiang Science and Technology Department Animal Experimental Research Project (2017C37141).

Compliance with Ethical Standards

All applicable international, national, and/or institutional guidelines for the care and use of animals were followed. All procedures performed in studies involving animals were in accordance with the ethical standards of the institution or practice at which the studies were conducted.

Conflict of Interest The authors declare that they have no conflict of interest.

References

1. Morice MC, Serruys PW, Sousa JE, Fajadet J, Ban Hayashi E, Perin M, et al. A randomized comparison of a sirolimus-eluting stent with a standard stent for coronary revascularization. N Engl J Med. 2002;346:1773–80.
2. Palmerini T, Benedetto U, Biondi-Zoccai G, Della Riva D, Bacchi-Reggiani L, Smits PC, et al. Long-term safety of drug-eluting and bare-metal stents: evidence from a comprehensive network meta-analysis. J Am Coll Cardiol. 2015;65:2496–507.
3. Inoue T, Node K. Molecular basis of restenosis and novel issues of drug-eluting stents. Circ J. 2009;73:615–21.
4. Kaul U, Bangalore S, Seth A, Arambam P, Abhaichand RK, Patel TM, et al. Paclitaxel-eluting versus everolimus-eluting coronary stents in diabetes. N Engl J Med. 2015;373:1709–19.
5. de la Torre Hernandez JM, Alfonso F, Martin Yuste V, Sanchez Recalde A, Jimenez Navarro MF, Perez de Prado A, et al. Comparison of paclitaxel and everolimus-eluting stents in st-segment elevation myocardial infarction and influence of thrombectomy on outcomes. Estrofa-im study. Rev Esp Cardiol (Engl Ed). 2014;67:999–1006.
6. Pan M, Burzotta F, Trani C, Medina A, Suarez de Lezo J, Niccoli G, et al. Three-year follow-up of patients with bifurcation lesions treated with sirolimus- or everolimus-eluting stents: seaside and corpal cooperative study. Rev Esp Cardiol (Engl Ed). 2014;67:797–803.
7. Joner M, Nakazawa G, Finn AV, Quee SC, Coleman L, Acampado E, et al. Endothelial cell recovery between comparator polymer-based drug-eluting stents. J Am Coll Cardiol. 2008;52:333–42.
8. Zhang DP, Ge YG, Ni ZH. Very late angiographic stent thrombosis after sirolimus-eluting stent implantation at 54 months. Zhonghua Xin Xue Guan Bing Za Zhi. 2008;36:176–7.
9. Takahashi S, Kaneda H, Tanaka S, Miyashita Y, Shiono T, Taketani Y, et al. Late angiographic stent thrombosis after sirolimus-eluting stent implantation. Circ J. 2007;71:226–8.
10. Kuriyama N, Kobayashi Y, Nakama T, Mine D, Nishihira K, Shimomura M, et al. Late restenosis following sirolimus-eluting stent implantation. JACC Cardiovasc Interv. 2011;4:123–8.
11. Kimura T, Morimoto T, Nakagawa Y, Kawai K, Miyazaki S, Muramatsu T, et al. Very late stent thrombosis and late target lesion revascularization after sirolimus-eluting stent implantation: five-year outcome of the j-cypher registry. Circulation. 2012;125:584–91.
12. Park SJ, Kang SJ, Virmani R, Nakano M, Ueda Y. In-stent neoatherosclerosis: a final common pathway of late stent failure. J Am Coll Cardiol. 2012;59:2051–7.
13. Shah R, Ramos-Bondy B, Mizeracki A. Risk of stent thrombosis with bioresorbable vascular scaffolds. Lancet. 2016;387:1903.
14. Poupon RE, Poupon R, Balkau B. Ursodiol for the long-term treatment of primary biliary cirrhosis. The udca-pbc study group. N Engl J Med. 1994;330:1342–7.
15. Rudolph G, Endele R, Senn M, Stiehl A. Effect of ursodeoxycholic acid on the kinetics of cholic acid and chenodeoxycholic acid in patients with primary sclerosing cholangitis. Hepatology. 1993;17:1028–32.
16. Luketic VA, Sanyal AJ. The current status of ursodeoxycholate in the treatment of chronic cholestatic liver disease. Gastroenterologist. 1994;2:74–9.
17. Lee CS, Kwon YW, Yang HM, Kim SH, Kim TY, Hur J, et al. New mechanism of rosiglitazone to reduce neointimal hyperplasia: activation of glycogen synthase kinase-3beta followed by inhibition of mmp-9. Arterioscler Thromb Vasc Biol. 2009;29:472–9.
18. Makino I, Tanaka H. From a choleretic to an immunomodulator: historical review of ursodeoxycholic acid as a medicament. J Gastroenterol Hepatol. 1998;13:659–64.
19. Vang S, Longley K, Steer CJ, Low WC. The unexpected uses of urso- and tauroursodeoxycholic acid in the treatment of non-liver diseases. Glob Adv Health Med. 2014;3:58–69.
20. Cho JG, Lee JH, Hong SH, Lee HN, Kim CM, Kim SY, et al. Tauroursodeoxycholic acid, a bile acid, promotes blood vessel repair by recruiting vasculogenic progenitor cells. Stem Cells. 2015;33:792–805.
21. Ma J, Nakajima T, Iida H, Iwasawa K, Terasawa K, Oonuma H, et al. Inhibitory effects of ursodeoxycholic acid on the induction of nitric oxide synthase in vascular smooth muscle cells. Eur J Pharmacol. 2003;464:79–86.
22. Lee WY, Han SH, Cho TS, Yoo YH, Lee SM. Effect of ursodeoxycholic acid on ischemia/reperfusion injury in isolated rat heart. Arch Pharm Res. 1999;22:479–84.
23. Kim SY, Kwon YW, Jung IL, Sung JH, Park SG. Tauroursodeoxycholate (tudca) inhibits neointimal hyperplasia by suppression of erk via pkcalpha-mediated mkp-1 induction. Cardiovasc Res. 2011;92:307–16.
24. Fan L, Chen LL, Lin CG, Peng YF, Zheng XC, Luo YK, et al. Firebird and cypher sirolimus-eluting stents and bare metal stents

in treatment of very long coronary lesions. Chin Med J. 2008;121: 1518–23.
25. Gao Z, Yang YJ, Chen JL, Qiao SB, Xu B, Qin XW, et al. Effects of sirolimus-eluting stent and the paclitaxel-eluting stent: a three-year follow-up study. Zhonghua Yi Xue Za Zhi. 2008;88:1811–4.
26. Gao H, Yan HB, Zhu XL, Li N, Ai H, Wang J, et al. Firebird sirolimus eluting stent versus bare mental stent in patients with st-segment elevation myocardial infarction. Chin Med J. 2007;120: 863–7.
27. Iaconetti C, De Rosa S, Polimeni A, Sorrentino S, Gareri C, Carino A, et al. Down-regulation of mir-23b induces phenotypic switching of vascular smooth muscle cells in vitro and in vivo. Cardiovasc Res. 2015;107:522–33.
28. Fitzgerald TN, Shepherd BR, Asada H, Teso D, Muto A, Fancher T, et al. Laminar shear stress stimulates vascular smooth muscle cell apoptosis via the akt pathway. J Cell Physiol. 2008;216:389–95.
29. Palumbo R, Gaetano C, Melillo G, Toschi E, Remuzzi A, Capogrossi MC. Shear stress downregulation of platelet-derived growth factor receptor-beta and matrix metalloprotease-2 is associated with inhibition of smooth muscle cell invasion and migration. Circulation. 2000;102:225–30.
30. Garanich JS, Pahakis M, Tarbell JM. Shear stress inhibits smooth muscle cell migration via nitric oxide-mediated downregulation of matrix metalloproteinase-2 activity. Am J Physiol Heart Circ Physiol. 2005;288:H2244–52.
31. Wang CF, Yuan JR, Qin D, Gu JF, Zhao BJ, Zhang L, et al. Protection of tauroursodeoxycholic acid on high glucose-induced human retinal microvascular endothelial cells dysfunction and streptozotocin-induced diabetic retinopathy rats. J Ethnopharmacol. 2016;185:162–70.
32. Chen S, Liu B, Kong D, Li S, Li C, Wang H, et al. Atorvastatin calcium inhibits phenotypic modulation of pdgf-bb-induced vsmcs via down-regulation the akt signaling pathway. PLoS One. 2015;10:e0122577.
33. Ikegami T, Matsuzaki Y. Ursodeoxycholic acid: mechanism of action and novel clinical applications. Hepatol Res. 2008;38:123–31.
34. Beuers U. Drug insight: mechanisms and sites of action of ursodeoxycholic acid in cholestasis. Nat Clin Pract Gastroenterol Hepatol. 2006;3:318–28.
35. Hua Y, Kandadi MR, Zhu M, Ren J, Sreejayan N. Tauroursodeoxycholic acid attenuates lipid accumulation in endoplasmic reticulum-stressed macrophages. J Cardiovasc Pharmacol. 2010;55:49–55.
36. Ozcan U, Yilmaz E, Ozcan L, Furuhashi M, Vaillancourt E, Smith RO, et al. Chemical chaperones reduce er stress and restore glucose homeostasis in a mouse model of type 2 diabetes. Science. 2006;313:1137–40.
37. Chen Y, Liu CP, Xu KF, Mao XD, Lu YB, Fang L, et al. Effect of taurine-conjugated ursodeoxycholic acid on endoplasmic reticulum stress and apoptosis induced by advanced glycation end products in cultured mouse podocytes. Am J Nephrol. 2008;28:1014–22.
38. Yanagitani K, Imagawa Y, Iwawaki T, Hosoda A, Saito M, Kimata Y, et al. Cotranslational targeting of xbp1 protein to the membrane promotes cytoplasmic splicing of its own mrna. Mol Cell. 2009;34: 191–200.
39. Zeng L, Li Y, Yang J, Wang G, Margariti A, Xiao Q, et al. Xbp 1-deficiency abrogates neointimal lesion of injured vessels via cross talk with the pdgf signaling. Arterioscler Thromb Vasc Biol. 2015;35:2134–44.
40. Ben Mosbah I, Alfany-Fernandez I, Martel C, Zaouali MA, Bintanel-Morcillo M, Rimola A, et al. Endoplasmic reticulum stress inhibition protects steatotic and non-steatotic livers in partial hepatectomy under ischemia-reperfusion. Cell Death Dis. 2010;1: e52.
41. Omar HR, Sprenker C, Karlnoski R, Camporesi EM, Mangar D. Late and very late drug-eluting stent thrombosis in the immediate postoperative period after antiplatelet withdrawal: a retrospective study. Ther Adv Cardiovasc Dis. 2014;8:185–92.
42. Franck C, Eisenberg MJ, Dourian T, Grandi SM, Filion KB. Very late stent thrombosis in patients with first-generation drug-eluting stents: a systematic review of reported cases. Int J Cardiol. 2014;177:1056–8.
43. Bechiri MY, Souteyrand G, Lefevre T, Trouillet C, Range G, Cayla G, et al. Characteristics of stent thrombosis in bifurcation lesions analysed by optical coherence tomography [J]. EuroIntervention. 2018;13(18):e2174–e2181.